

A millennial summer temperature reconstruction for northeastern Canada using oxygen isotopes in subfossil trees

M. Naulier¹, M.M. Savard², C. Bégin², F. Gennaretti⁴, D. Arseneault⁴, J. Marion², A. Nicault³, Y. Bégin¹

¹ Institut national de la recherche scientifique-ETE, 490 rue de la Couronne, QC, G1K9A9, Canada

² Geological Survey of Canada, Natural Resources Canada, 490 rue de la Couronne, QC, G1K9A9, Canada

³ Aix-Marseille University, ECCOREV (FR-3098), Europôle Méditerranéen de l'Arbois, BP 80, 13545 Aix-en-Provence cedex 4, France

⁴ Université du Québec à Rimouski, 300 allée des Ursulines, Rimouski, G5L3A1, Canada

Abstract

Climatic reconstructions for north-eastern Canada are scarce such that this area is under-represented in global temperature reconstructions. To fill this lack of knowledge and identify the most important processes influencing climate variability, this study presents the first summer temperature reconstruction for eastern Canada based on a millennial oxygen isotopic series ($\delta^{18}\text{O}$) from tree rings. For this purpose, we selected 230 well-preserved subfossil stems from the bottom of a boreal lake and five living trees on the lakeshore. The sampling method permitted an annually resolved $\delta^{18}\text{O}$ series with a replication of five trees per year. The June to August maximal temperature of the last millennium has been reconstructed using the statistical relation between Climatic Research Unit (CRU TS3.1) and $\delta^{18}\text{O}$ data. The resulting millennial series is marked by the well-defined Medieval Climate Anomaly (MCA; AD 1000-1250), the Little Ice Age (AD 1450-1880) and the modern period (AD 1950-2010), and an overall average cooling trend of $-0.6^\circ\text{C}/\text{millennium}$. These climatic periods and climatic low frequency trends are in agreement with the only reconstruction available for northeastern Canada and others from nearby regions (Arctic, Baffin Bay) as well as some remote regions like the Canadian Rockies or Fennoscandia. Our temperature reconstruction indicates that the Medieval Climate Anomaly was characterized by a temperature range similar to the one of the modern period in the study region. However, the temperature increase during the last three decades is one of the fastest warming observed over the last millennium ($+1.9^\circ\text{C}$ between 1970-2000). An additional key finding of this research is that the coldest episodes mainly coincide with low solar activities and the extremely cold period of the early 19th century has occurred when a solar minimum was in phase with successive intense volcanic eruptions. Our study provides a new perspective unraveling key mechanisms that controlled the past climate shifts in northeastern Canada.

34 1. Introduction

35

36 The recently published work of the Intergovernmental Panel on Climate Change (IPCC AR5,
37 2013; PAGES 2K consortium, 2013) has shown that north-eastern Canada is poorly
38 represented among existing millennial temperature reconstructions in the northern
39 hemisphere. For this reason, a better knowledge of regional past climate variations registered
40 in natural archives is needed. The use of natural archives such as trees, sediment or pollen
41 has permitted the reconstruction of temperature variability at regional, hemispheric and global
42 scales for the past millennium (Hegerl *et al.*, 2007; Mann *et al.*, 2009; Moberg *et al.*, 2005;
43 PAGES 2k consortium, 2013). Although some studies have documented past climatic
44 conditions in northern Canada (Moore *et al.*, 2001; Thomas and Briner, 2009; Luckman and
45 Wilson, 2005; Edwards *et al.*, 2008; Viau and Gajewski, 2009; Gajewski and Atkinson, 2003),
46 only one annually-resolved millennial temperature reconstruction based on tree-ring widths
47 exists for eastern Canada (Gennaretti *et al.*, 2014; summer temperature reconstruction for
48 Eastern Canada, STREC), but none has been based on the isotopic approach. Consequently,
49 obtaining millennial-long, high-resolution temperature reconstructions from additional proxies
50 in north-eastern Canada is important to increase our knowledge of the past climate, and
51 better understand the mechanisms of climate change.

52 Tree-ring isotope series present the advantage that they generally do not need to be
53 detrended; they retain climatic low frequency variations, and require fewer trees compared to
54 classical dendrological methods (Loader *et al.*, 2013; Robertson *et al.*, 1997; Young *et al.*,
55 2010). Moreover, oxygen ($\delta^{18}\text{O}$) and carbon ($\delta^{13}\text{C}$) series have proven their suitability for
56 reconstructing past summer temperatures (Anchukaitis *et al.*, 2012; Barber *et al.*, 2004; Daux
57 *et al.*, 2011; Luckman and Wilson, 2005; Porter *et al.*, 2013). Whereas $\delta^{13}\text{C}$ series have often
58 been used for long climatic reconstructions, only a few studies have used long $\delta^{18}\text{O}$ series
59 (Edwards *et al.*, 2008; Richter *et al.*, 2008; Treydte *et al.*, 2006; Wang *et al.*, 2013). A
60 previous study has already proven that $\delta^{18}\text{O}$ is the most suitable isotopic proxy for summer
61 temperature reconstruction in our study region (Naulier *et al.*, 2014; Naulier *et al.*, in press).

62 In northern Canada, most tree species rarely live more than 300 years (Arseneault *et al.*,
63 2013). In such regions where old trees are missing, isotopic chronologies can be extended by
64 combining living specimens with subfossil trees preserved in lakes (Boettger *et al.*, 2003;

65 Gagen *et al.*, 2012; Mayr *et al.*, 2003; Savard *et al.*, 2012), and cross-dating stems to
66 determine subfossil tree ages (Arseneault *et al.*, 2013). For the purpose of paleoclimate
67 studies, subfossil stems can be easily extracted and collected from large stocks of drowned
68 subfossil logs in lakes and can be associated with specific edaphic contexts as most
69 specimens are not redistributed in lakes (Gennaretti *et al.*, 2014a).

70 After cross-dating, the development of a robust millennial, isotopic chronology from the
71 combination of living and subfossil stems involves replicating specimens in order to retain the
72 climate variability of the study site (Haupt *et al.*, 2014; Loader *et al.*, 2013a). However, the
73 amount of material available is often a constraint because of the short lifespans of trees, the
74 difficulty to separate single and thin rings and obtaining enough cellulose for isotopic analysis
75 (Loader *et al.*, 2013b; Boettger and Friedrich, 2009). To overcome these problems, different
76 sub-sampling methods have been developed such as tree pooling (McCarroll and Loader,
77 2004; Dorado Liñán *et al.*, 2011), serial pooling of consecutive tree rings within an individual
78 tree (Boettger and Friedrich, 2009), and the “offset-pool plus join-point method” (Gagen *et al.*,
79 2012). This last method has permitted constructing a millennial $\delta^{13}\text{C}$ series with annual
80 resolution and high replication, while reducing the sampling efforts and laboratory analyses
81 (Gagen *et al.*, 2012). Moreover, a statistical analysis of this method has confirmed its
82 robustness and possible application for the production of millennial $\delta^{18}\text{O}$ series (Haupt *et al.*,
83 2014).

84 The present study aims to produce a new paleoclimatic data set based on tree-ring $\delta^{18}\text{O}$
85 series covering the last millennium in northeastern North America. For this purpose, we
86 develop a 1010-years long $\delta^{18}\text{O}$ series using a combination of living trees and submerged
87 subfossil stems from one site, and reconstruct the summer maximal temperature. We analyze
88 the main characteristics of the climatic series and evaluate its robustness by comparison with
89 other reconstructed temperature series. Finally, we explore the potential impact of natural
90 forcing (solar radiation and volcanic eruptions) on past climatic variability in north-eastern
91 Canada.

92

93 **2. Materials and methods**

94

95 **2.1. Study area**

97 The study site is located at the center of the Quebec-Labrador peninsula in north-eastern
98 Canada (Figure1A). This area is part of the Precambrian Canadian Shield, mainly constituted
99 of granitic and gneissic rocks. The landscape is characterized by a low altitude plateau (400-
100 600 m), with abundant lakes and wetlands (Dyke *et al.*, 1989). Forests of the area are
101 dominated by black spruce (*Picea mariana* (Mill.) BSP) trees, developed as pure open lichen
102 woodlands on well-drained sites, and spruce-moss woodlands in depressions. Balsam fir
103 (*Abies balsamea* (L.) Mill.) and Tamarack (*Larix laricina* (Du Roi) Koch) also grow in this
104 region. Wildfires are the most important natural disturbances with a rotation period estimated
105 between 250 to 500 years (Boulanger *et al.*, 2012).

106 The climate is continental and subarctic with short, mild summers and long, cold winters.
107 Environment Canada data (Schefferville station) show that the 1949 to 2010 mean monthly
108 temperature is -22.9°C in January and 13.3°C in July with a mean annual temperature of -
109 3.9°C. Total annual precipitation averaged 640 mm with up to 60% falling in summer (June to
110 September). The mean duration of the frost-free period is 75 days from mid-late June to mid-
111 September. The lakes are generally frozen from mid-October to early June.

112 The selected lake (L20; 54°56'31" N; 71°24'10" W) is part of the large network of lakes
113 sampled by our group (Arseneault *et al.*, 2013; Gennaretti *et al.*, 2014a and b). Ecological and
114 morphological criteria have been developed to identify lakes that present the best potential for
115 millennial-long climatic reconstructions (well-preserved subfossil trees) and large stocks of
116 subfossil logs. These lakes are typified by an abrupt lake/forest transition, as well as log
117 accumulation in the lower littoral zone away from ice erosion and waves (Arseneault *et al.*,
118 2013, Gennaretti *et al.*, 2014a, Gennaretti *et al.*, 2014c). Lake L20 has an altitude of 483 m
119 and an area of 35.1 ha. It is bordered by open spruce-moss with lichen woodlands growing on
120 well-drained podzolic soil and regular slope. The last severe wildfire occurred at about AD
121 1590 along the southern section of the studied shore segment and more than 1200 years ago
122 along the northern section (Gennaretti *et al.*, 2014c).

123

124 2.2. Tree stem selection and sampling strategy

125

126 We recently demonstrated that isotopic series from different heights along lakeshore trees
127 provide similar isotopic trends, and indicated that the combination of lakeshore black spruce
128 trees with subfossil stem segments does not introduce artefacts in long $\delta^{18}\text{O}$ series, thus
129 permitting their combination for climatic reconstruction (Naulier *et al.*, 2014). In the present
130 study, subfossil stems were selected from a large collection of 586 cross-dated specimens
131 from lake L20, also used in the STREC reconstruction (Gennaretti *et al.*, 2014b), based on
132 their excellent degree of preservation (Savard *et al.*, 2012), relatively large ring width (>0.2
133 mm) and their life span (Supplementary material, Table I). The development of a millennial
134 isotopic series requires choosing an appropriate method to preserve both high and low
135 climate frequencies, while limiting analytical efforts. We decided to adapt the “offset-pool plus
136 join-point method” (Gagen *et al.*, 2012) in order to obtain an annual resolution with a
137 replication of five trees for each year.

138 According to this sampling method, one cohort is made by selecting segments from five
139 contemporaneous trees such that each cohort overlaps the next one over five years. In our
140 case, five living trees were selected to construct a modern cohort (CV; AD 1860-2006) and 60
141 well-preserved subfossil stems from the lake floor were used to produce 12 subfossil cohorts
142 (C0 to C11; AD 997-1956; Figure 2). Overall, our cohorts cover between 59 and 111-years
143 and the complete suite of cohorts extends from AD 997 to 2006. Additionally, within every
144 cohort, each tree was divided into five-year blocks which were offset by one year among trees
145 (Supplementary material, Table II). As a consequence, the $\delta^{18}\text{O}$ value obtained for a specific
146 year is the mean of the isotopic results from five trees, which represents a triangular
147 centralized nine-year moving average.

148

149 2.3. Laboratory treatment

150

151 We extracted α -cellulose sub-samples according to a standard protocol modified for small
152 samples at the Delta-lab of the Geological Survey of Canada (Green, 1963; Savard *et al.*,
153 2012). The extracted α -cellulose was dried at 55°C for 12 hours and sub-samples analyzed
154 using peripherals on-line with gas-source isotope ratio mass spectrometers (IRMS). All
155 material was analyzed for $\delta^{18}\text{O}$ values with a pyrolysis-CF-IRMS (Delta plus XL). The
156 analytical accuracy of this instrument was 0.2‰ (1 σ), as established by using international

standards (IAEA-SO-6 and IAEA-NBS-127). All $\delta^{18}\text{O}$ measures are reported in permil (‰) relative to the Vienna Standard Mean Ocean Water (VSMOW). A total of 2192 analyses were produced, with, in addition, 24% of all samples retreated and analyzed to determine the external precision (reproducibility) of the complete procedure (0.2‰, 1σ).

161

2.4. Cohort corrections and climatic reconstruction

163

When a long isotopic series is produced from trees coming from a random assemblage, joining two successive cohorts may be difficult due to the existence of isotopic offsets between cohorts. An approach to overcome this problem is to use the mean of $\delta^{18}\text{O}$ values coming from several tree segments from the overlap period between two successive cohorts that permit to estimate a correction factor for the offset (Gagen *et al.*, 2012). In the present study, the construction of the millennial $\delta^{18}\text{O}$ series required such an adjustment for some cohorts. We have adopted the “join-point method” proposed by Gagen *et al.* (2012). A join-point (hereafter JP), corresponds to the mean results of 5-year blocks from several trees overlapping between two cohorts. We have used all available dated trees (between 10 and 24) to produce the required join points (JP 0 to JP 11), and verified several methods to correct for the offsets between cohorts. Hence, every cohort has been corrected by adding the linear regression calculated between the $\delta^{18}\text{O}$ values of its two ends.

The integrity of the isotopic signal has been verified elsewhere (Naulier, 2015). The $\delta^{18}\text{O}$ values of lignin and cellulose have been analyzed for three contrasted climatic periods of the millennium (AD. 1141-1164, 1741-1761 and 1886-1909), as detected in previous studies (e.g. Savard *et al.*, 2012). The cellulose isotopic integrity of the subfossil stems has been confirmed by the similarity of the Δ values between living trees and subfossil stems for the 1886-1909 period. In addition, the departure between the $\delta^{18}\text{O}$ values of lignin and cellulose ($\Delta = \delta^{18}\text{O}_{\text{cellulose}} - \delta^{18}\text{O}_{\text{lignin}}$) exhibit no temporal trend.

In previous studies, we have analyzed the relationships between $\delta^{18}\text{O}$ series of five living trees and various climatic parameters (temperature, precipitation, vapor pressure deficit, etc.). We have established that $\delta^{18}\text{O}$ series of black spruce stems sampled at an annual resolution from boreal lakeshore were significantly correlated with June-August (JJA) maximal

187 temperature (Tmax; $r=0.54$). We have also determined by statistical analysis (Buishand test,
188 Buishand, 1982) that the summers became warmer after 1975 and that the growing season
189 duration and degree-days have increased importantly during the last decade (2000-2010).
190 Moreover, we have demonstrated that during this decade the growing season started sooner
191 and finished later than before, changing the relationship between JJA maximal temperature
192 and $\delta^{18}\text{O}$ series (divergence). In other words, this JJA Tmax and $\delta^{18}\text{O}$ series relation is stable
193 and strong between 1930 and 2000 ($r_{\text{mean}} = 0.54$; 1930-2000), but not after (AD 2000-2010;
194 Naulier *et al.*, 2014; Naulier *et al.*, in press). Therefore, in the present study, we excluded the
195 last decade (divergent years) when calibrating the $\delta^{18}\text{O}$ series on temperature data which is
196 assumed to be non-representative of the temperature variation over the last century. The
197 $\delta^{18}\text{O}$ series of subfossil cohorts are filtered on 9 years; we have made the choice to pass a 9-
198 year centered-filter on the JJA maximal temperature CRU TS 3.1 in order to use series all
199 treated in the same way for the reconstruction.

200 In a first step, a simple linear regression and a linear-scaling model were calibrated over
201 the entire 1930-2000 period with climatic data. Climate data from the 1900-1929 period were
202 excluded because no meteorological station was then operating at less than 300 km from the
203 study site. The climatic series was separated into two equal periods (AD 1930-1970 and
204 1971-2000; Table 1) in order to test the robustness of the two calibration models, using the
205 non-first-differenced reduction of error (RE), the coefficient of error (CE), the raw mean
206 squared error (RMSE) and the coefficient of determination (r^2). The linear regression and the
207 linear-scaling calibration procedures resulted in somewhat different temperature
208 reconstructions of similar robustness with similar RE, CE, r^2 and RMSE coefficients. In both
209 cases, the model residuals satisfy the standard linear regression assumptions of normality,
210 variance and autocorrelation (not shown), but cannot reproduce all attributes of the measured
211 data. We therefore tested the possibility of averaging the two model results, and this option
212 gave the best reproduction of the measured Tmax. Consequently, we averaged results from
213 the two reconstructions in order to obtain one robust reconstruction (Table 1; Supplementary
214 material, Table III).

215 Then, i-STREC was compared to the only other regional temperature reconstruction
216 (STREC; Gennaretti *et al.*, 2014), which is built from ring width data from 6 lakes, including
217 our site, and with reconstructions based on tree rings from another boreal region
218 (Fennoscandia, Helama *et al.*, 2002; Figure). We also compared i-STREC with independent

219 temperature reconstructions based on other natural archives from North America and the
220 Arctic region (Thomas and Briner, 2009; Kobashi *et al.*, 2011; Luckman and Wilson, 2005;
221 Vinther *et al.*, 2009, Figure 5). Most published reconstructions are based on mean
222 temperatures, except our reconstruction and the one from the Canadian Rockies, which are
223 based on summer maximal temperatures. The influence of climatic forcings was evaluated
224 through the comparison of i-STREC with time series of sulfate emission from volcanic origin
225 (Crowley *et al.*, 2012) and solar radiation series (Bard *et al.*, 2003; Figure 6). The durations of
226 the solar minima have been determined according to existing estimations of solar radiation
227 (e.g., Bard *et al.*, 2003).

228

229 3. Results and discussion

230

231 3.1. Development of $\delta^{18}\text{O}$ chronology

232

233 As the purpose of the reconstruction was to identify contrasted periods and important
234 temperature changes over the last millennium, the choice of the sampling method proposed
235 by Boettger *et al.* (2009) was relevant because it allows for reconstruction of climatic
236 parameters at an annual resolution with a replication of five trees per year. The range of $\delta^{18}\text{O}$
237 values of trees is between 19.5 and 22.0‰, and the largest $\delta^{18}\text{O}$ differences among trees
238 within a junction is obtained for JP5 (3.8‰; Figure 3A). This large inter-tree variability can be
239 explained by a combination of causes, including different growing locations along the
240 lakeshore which influence the water supply of trees (Figure 1B), and inter-tree metabolic
241 variability (0.5‰ in Naulier *et al.*, 2014). Such variability confirms the need to take a large
242 number of trees for a millennial reconstruction in order to capture the site signal (Loader *et al.*,
243 2013a).

244 The $\delta^{18}\text{O}$ values at intersections between two successive cohorts and of the JP $\delta^{18}\text{O}$
245 means are surprisingly matching in most cases (except at the C8/C9 and C3/C4 junctions;
246 figure 3). These observations suggest that offset correction between cohorts is not always
247 necessary. However, we have determined that a modification of the JP adjustment procedure
248 published by Gagen *et al.* (2012) would optimize the correction while conserving the isotopic

249 variability and trends over the millennium (Naulier, 2015). Hence, we have used the mean of
250 $\delta^{18}\text{O}$ values of JP from overlapping cohorts to calculate the required adjustment, this mean
251 being considered as “the adjustment value”. Correcting cohort $\delta^{18}\text{O}$ series with this method
252 increases the number of trees considered (20 to 33 trees instead of 10 to 23 trees if only JP
253 are used). After correction, the mean of the millennial $\delta^{18}\text{O}$ series is 20.8‰. The strong
254 correlation between the $\delta^{18}\text{O}$ series of living trees and subfossil stems ($r^2=0.70$) over their
255 overlapping period (1860-1956) confirms the isotopic integrity of the subfossil stems, and
256 ensures that the climatic reconstruction can be performed over the rest of the millennial $\delta^{18}\text{O}$
257 series.

258 Although the cohort sampling method presents many positive points, it is important to
259 highlight some of its flaws. Indeed, the sampling strategy produces a $\delta^{18}\text{O}$ series smoothed
260 with a centered 9-year filter. This smoothing leads in some cases to series requiring more
261 precaution than non-smoothed series before they can be interpreted or used. For instance,
262 the calibration of our smoothed $\delta^{18}\text{O}$ series required a centered 9-year filtering of the climatic
263 series. Consequently, correlations between isotopic and climatic series are improved by
264 smoothing due to the sampling method. Nevertheless, these correlations represent solid and
265 real links, and do not create artefacts (see also section 3.2.1, and Naulier *et al.*, 2014).

266

267 3.2. Model validation and millennial climatic reconstruction

268

269 3.2.1. Model validation

270

271 We have compared two methods of sampling and production of the ring series from living
272 trees prior to calibration: (1) separation at an annual resolution without pooling (e.g., Haupt *et*
273 *al.*, 2013); and (2) sampling with the cohort approach. We have found that the second was
274 best suited because it slightly improved the correlation between $\delta^{18}\text{O}$ series and maximal
275 temperatures ($r^2=0.64$ vs 0.54 with annual resolution), and it allows using $\delta^{18}\text{O}$ series
276 compatible with the one used for the millennial subfossil series (9-year moving average).
277 Consequently, the $\delta^{18}\text{O}$ series of the living-tree cohort (CV) was used to calibrate the model
278 and to provide a robust reconstruction as it show a strong correlation with the new CRU
279 series ($r^2=0.64$) for the entire calibration period (1930-2000), which confirmed that the

280 reconstruction of past temperature with the average $\delta^{18}\text{O}$ series is suitable (Figure 4A). The
281 RMSE is 0.26, with a RE and a CE of 0.60. However, it appears that the calibration and
282 verification coefficients are significantly changing depending on the period selected for the
283 statistical analysis. This observation implies that the correlation between Tmax and $\delta^{18}\text{O}$
284 series is not stable over the last century even if the correlation stays significant (Naulier *et al.*
285 in press).

286 These statistical results confirm that the summer temperature reconstructed based on $\delta^{18}\text{O}$
287 values (i-STREC) are representative of the natural variability that existed in north-eastern
288 Canada.

289

290 3.2.2. Millennial temperature trends in north-eastern Canada

291

292 The i-STREC shows a 0.6°C decrease of maximum summer temperature over the past
293 millennium (Figure 4B), whereas a millennial 0.2°C cooling is roughly estimated for the mean
294 temperature of northern hemisphere (PAGES 2k consortium, 2013). However, our local
295 temperature decrease is in the same order of magnitude as the decrease of summer-months
296 mean temperature reconstructed using pollen in the North American tundra (Viau *et al.*,
297 2012), and in northern regions of high latitudes (sediment, tree-ring widths, ice core in
298 Kaufman *et al.*, 2009 and tree-ring widths in Esper *et al.*, 2012). This temperature decline
299 over the last millennium is generally attributed to orbital forcing (PAGES 2k consortium,
300 2013).

301 The reconstruction suggests that the maximum summer temperature has varied from a
302 maximum of 17.3°C around AD 1008-1010 to a minimum of 14.8°C around AD 1670-1674.
303 The twentieth century was generally cold (mean of 16°C) with an abrupt warming trend during
304 the last three decades (+0.2°C/10 years between AD 1900-1980 and +0.8°C/decade between
305 AD 1980-2010; CRU TS 3.1 data; Figure 4A). Furthermore, two major climatic episodes were
306 also revealed by i-STREC: a warm period during the eleventh and twelfth centuries (mean of
307 16.5°C between 1000 and 1250) and a cold period from the early fifteenth to the end of the
308 nineteenth centuries (mean of 15.8°C between 1450 and 1880; Figure 4B). These periods are
309 in agreement with the general knowledge of the temperature trends observed globally for the
310 last millennium and correspond to the Medieval Climate Anomaly (MCA) and the LIA,

311 respectively (IPCC 2013, PAGES 2k consortium, 2013). Based on i-STREC data, we
312 associate these two climatic episodes to the ~ AD 1000-1250 and ~ AD 1450-1880 time
313 periods, respectively.

314

315 3.2.3. Evidences of contrasted climatic periods

316

317 The high summer temperatures of the 11th century (AD ~ 1000-1250; Figure 4B) coincide
318 with peaks previously observed in our study area based on tree-ring width (Gennaretti *et al.*,
319 2014b; STREC), as well as in Greenland ice cores (Kobashi *et al.*, 2011; Vinther *et al.*, 2009,
320 2010), tree-ring series from the Canadian Rockies (Luckman and Wilson, 2005) and
321 Fennoscandia (Helama *et al.*, 2002; Figure 5), and large-scale reconstructions (Mann *et al.*,
322 2009, Ljungqvist *et al.*, 2012, Kaufman *et al.*, 2009, Trouet *et al.*, 2013). Several hypotheses
323 on the forcing of this warm anomaly have been proposed, including a prolonged tendency
324 towards a positive-phase of the North Atlantic Oscillation (NAO; Trouet *et al.*, 2009; Trouet *et al.*,
325 2012) or a synchronicity between La Niña phase and a warm phase in the Atlantic
326 Multidecadal Oscillation (AMO; Feng *et al.*, 2011; Mann *et al.*, 2009). In northeastern Canada,
327 the NAO has an important impact on winter temperatures but not for summer (Hurrell *et al.*,
328 2003). In contrast, the AMO influences spring and summer temperatures (Fortin and
329 Lamoureux, 2009) and is partly responsible for the recent sea surface temperature warming
330 of northeastern Canada (Ding *et al.*, 2014). However, the state of the AMO at the beginning of
331 the millennium and its potential influence on climate during the MCA are unknown. Recently,
332 Sicre *et al.* (2014) have demonstrated that during the MCA, the Northern Annular Mode
333 (NAM) was effective concomitantly with a strong ice-loaded Labrador Current (LC). This
334 combination could be responsible for a decrease of fresh air from the Arctic to eastern
335 Canada, and consequently, for an increased temperature along the continent.

336 Following the MCA, i-STREC emphasizes a cold period between ~ AD 1450 and 1880,
337 which can be attributed to the Little Ice Age (LIA; Figure 4B). It is worth noting that a short
338 warming phase occurred between 1510 and 1590 (Figure 4B). Such warm phase also
339 occurred at the eastern Canadian treeline and included the expansion of upright tree growth
340 forms in lichen-spruce woodland (Payette *et al.*, 1989). Overall, the LIA is recorded in several
341 Northern hemisphere temperature reconstructions based on various proxies, even if its length

342 vary among regions (PAGES 2k consortium, 2013). At the hemispheric scale, the LIA is a
343 well-documented cool period (Moberg *et al.*, 2005; Mann *et al.*, 2009; Hegerl *et al.*, 2007), and
344 several causes may have concurred to trigger its occurrence, including a succession of strong
345 volcanic eruptions (Crowley, 2000; Miller *et al.*, 2012, Gennaretti *et al.*, 2014b), millennial
346 orbital cooling (Kaufman *et al.*, 2009; Esper *et al.*, 2012), and low solar radiation (Bard *et al.*,
347 1997).

348 It is without surprise that the MCA was warmer than the LIA ($+0.4\pm0.3^{\circ}\text{C}$) in the L20 area.
349 We have furthermore compared maximal temperature of the MCA with the modern warming,
350 following the approach used in the IPCC report (Masson-Delmotte *et al.*, 2013). The running
351 50-years averages between 1000 and 1100 were higher ($+0.2\pm0.1^{\circ}\text{C}$) than the measured
352 temperature of the last 50 years (1959-2009). It is worth nothing that when considering 30-
353 years running averages, the 1979-2009 period appears to be the warmest (average of
354 $+0.6^{\circ}\text{C}\pm0.4$) over the last millennium. Considering these results, one can infer that the MCA
355 and recent warming show similar average maximal temperature in the study area.

356 These results contrast somewhat with Northern hemisphere temperature reconstructions
357 that have determined that the mean annual temperature of the modern period was the
358 warmest in northern Canada (Mann *et al.*, 2009; Ljungqvist *et al.*, 2012). Indeed, the data
359 available for these hemispheric reconstructions in the last IPCC report are scarce for north-
360 eastern Canada (Viau *et al.*, 2012). Clearly, the i-STREC results indicate that the MCA in
361 northeastern Canada has been as warm as the modern period of the last millennium (Figure
362 5). The similarities between MCA and the modern period were expected considering that the
363 MCA has been widely studied for its similarities with the modern warming period.
364 Nevertheless, the causes that triggered these similar climatic periods are likely different (i.e.,
365 Landrum *et al.*, 2013; Way and Viau, 2014). Indeed, if the MCA is solely controlled by natural
366 processes, it seems that the warming during the modern period results from a combination of
367 natural and anthropogenic causes (i.e., Mann *et al.*, 2009; Viau *et al.*, in press). By using
368 empirical statistical modeling and global climate models for the 1881-2011 period in Labrador,
369 Way and Viau (2014) have shown that up to 65% of the variance in annual air temperature
370 was explained when also including anthropogenic forcing in the model. Even if summer
371 temperature has increased at a lower rate compared to annual air temperature in Labrador,
372 the observed warming ($+1.9^{\circ}\text{C}$) between 1970 and 2000 in the region of L20 is one of the

373 fastest over the last millennium. In the next decades, if warming continues at this rate,
374 temperature will reach a new record for the last millennium.

375

376 3.2.4. Climatic forcings of the last millennium

377

378 Contrary to previous studies, our isotopic series does not emphasize an abrupt LIA onset in
379 response to volcanic forcing such as the AD 1257 Samalas event (Lavigne *et al.*, 2013;
380 Figure 6). Instead, our data suggest that solar radiation was the most influential forcing on
381 Tmax changes in the studied region. Indeed, the most important cooling phases of i-STREC
382 occurred during periods of low solar activity like the Oort (AD 1040-1080), Dalton (AD 1800-
383 1850), Maunder (AD 1600-1650) and Spörer (AD 1410-1480) minima (Figure 6). A simple re-
384 sampling method involving 1000 iterations of re-sampling (bootstrapped) has demonstrated
385 that the low temperature periods were always associated to low solar radiation periods
386 ($p < 0.05$). Proposing that solar radiation represents an important control on temperature in
387 north-eastern Canada is in agreement with the hypothesis that the solar forcing was important
388 during the last millennium (AD 1000 to ~1900), except during the modern period
389 (Breitenmoser *et al.*, 2012; Keller *et al.*, 2004), implying that recent anthropogenic impact is
390 the main control at that time. However, even i-STREC is not significantly influenced by
391 volcanism, as determined by superimposed epoch analysis (results not shown), the possibility
392 that successive strong volcanic eruptions combined with solar minima could have contributed
393 to the important LIA cooling in Northeastern Canada cannot be discarded. Strong eruptions
394 and solar minima coincide during the Maunder minimum with the Kuwae eruption, and the
395 Dalton minimum with the unknown (1809), Tambora (1815) and Cosiguina (1835) eruptions.
396 The role of coinciding natural forcings is also invoked in other paleoclimatic studies that have
397 compared northern hemisphere reconstructions with solar radiation series (e.g., Bard *et al.*,
398 2006; Breitenmoser *et al.*, 2012; Crowley *et al.*, 2000; Lean *et al.*, 1995; Shindell *et al.*, 2003).
399 These studies have shown that temperature changes were largely due to solar forcing alone
400 during the first part of the last millennium, and to volcanic and solar forcings (i.e.,
401 Breitenmoser *et al.*, 2012), or to volcanic eruptions (i.e., Crowley *et al.*, 2000; Keller *et al.*,
402 2004) during the end of the LIA (after 1600). In addition, Tingley *et al.* (2014) have
403 demonstrated, by analyzing the ring density in trees growing at high latitude, that the trees

404 recorded not only volcanic eruptions but also variations in light intensity. This finding indicates
405 that both isotopes and density of trees can record changes in solar radiations.

406 The other temperature reconstruction produced for the studied region (STREC) contains a
407 stronger volcanic signal than i-STREC (Gennaretti *et al.*, 2014b). Considering that the two
408 reconstructions are statistically robust, we can assume that they both reflect real trends. In
409 addition, calibrating STREC using the same approach than for i-STREC (i.e. calibration on
410 maximum temperature over the 1930-2000 time period) indicates that methods cannot
411 account for the main differences between the two reconstructions. Consequently, differences
412 in thermal trends between i-STREC and STREC must be caused by their respective
413 sensitivity to climatic triggers and control mechanisms, ring width and $\delta^{18}\text{O}$ values. The first
414 important point to bear in mind is that temperature is the main control on changes in ring
415 widths and $\delta^{18}\text{O}$ values, but not the only one. Consequently, other climatic parameters (i.e.,
416 precipitations, vapor pressure deficit) have also generated short and medium variations on
417 the two series, creating an important “climatic noise” at high and medium frequencies,
418 possibly explaining the differences between the reconstructions (Naulier *et al.*, 2014).
419 However, the ring width and $\delta^{18}\text{O}$ series used to generate STREC and i-STREC display
420 similar long-term climatic trends. This last point is quite important, considering that our main
421 purpose was to identify long climatic tendencies over the last millennium in northeastern
422 Canada.

423 The second important aspect to consider is that the temperature-linked processes
424 responsible for the variations of ring widths and $\delta^{18}\text{O}$ values slightly differ. In the studied
425 region, rings widths are directly influenced by photosynthetic rates, which generally increase
426 with ambient temperatures. In addition, volcanic aerosols blocking light after a major volcanic
427 eruption may also reduce ring growth concomitantly to reduced temperature, explaining the
428 strong influence of major volcanic events on ring width. In contrast, one of the main controls
429 on the final tree-ring $\delta^{18}\text{O}$ values is the temperature prevailing regionally during cloud mass
430 distillation, as registered in the raindrop signal and transferred to the source water in soils,
431 then through the root system, to the tree. Moreover, the temperature effects on fractionation
432 during distillation and precipitation (Rayleigh process) are not limited to a temperature range,
433 and may record temperature lows modulated by solar minimums. When strong volcanic
434 events are combined with minimal solar radiations, the strong influence on regional
435 temperature is therefore detected by $\delta^{18}\text{O}$ values of rain drops. These key differences in

mechanisms controlling temperature recorded in ring widths and $\delta^{18}\text{O}$ values imply that the two proxies may emphasize forcings in a complementary way.

As a summary, it appears that ring widths or $\delta^{18}\text{O}$ series have strengths and weaknesses as proxy of past climatic conditions. However, the climatic data that can be extracted from the two series can generate complementary information, permitting to highlight several climatic forcings and identify the main regional control on past, present and future temperatures. Nevertheless, there are still needs for further understanding the differences between processes influencing isotopic assimilation and ring-width growth. Such information would be useful for future climatic reconstruction using a multi-indicator approach.

4. Conclusion

1. The cohort sampling method allows reconstructing climatic variability of medium and low frequencies by using fewer samples than other sampling methods, with a high temporal resolution and analytical replication. Our adjustment of the method of joining cohorts, the JP-adjustment method, permits the preservation of $\delta^{18}\text{O}$ variability between segments of trees without biasing the millennial $\delta^{18}\text{O}$ series.

2. The combination of two statistical models (linear scaling and simple linear regression) has permitted an adequate reproduction of the measured regional temperature, and allowed reconstructing maximum temperature over the last millennium.

3. i-STREC is complementary to the only other reconstruction in the study region (STREC, based on tree-ring width). These two reconstructions should be combined within a multi-parameter approach to increase the proportions of variance explained.

5. i-STREC suggests that the main climatic forcing at play during the last millennium in the studied region was solar activity, but we remain cautious because we base this hypothesis solely on an apparent correlation between reconstructed Tmax and the curve for solar radiations. Clearly, coldest episodes in the L20 area coincide with low solar radiation (Oort, Spörer, Maunder and Dalton), with the exception of an episode in the nineteenth century,

465 during which low solar radiations (Dalton minima) were combined with two successive and
466 strong volcanic eruptions (unknown 1809 and Tambora 1815 eruptions).

467 6. Overall, i-STREC shows that the Medieval Climate Anomaly (997-1250) was characterized
468 by a temperature range similar to the one of the modern period in the study region. However,
469 the sudden and rapid temperature increase during the last three decades is one of the fastest
470 over the last millennium (+1.9°C between 1970 and 2000) and if this rapid warming rate
471 persists, the future climate in northeastern Canada may become an issue of concern.

472 **Acknowledgments**

473 The authors would like to thank Anna Smirnoff, Marie-Christine Simard and Marc Luzincourt
474 for their technical support during sample treatment and analyses at the Delta-Lab of the
475 Geological Survey of Canada. We are grateful to Julia Autin, Pierre-Paul Dion and Yves
476 Bouthillier for the sampling of lakeshore trees and subfossil stems. We also would like to
477 thank Dr. Steve Wolfe who made constructive comments during a pre-submission review of
478 this article. This research was supported financially by the NSERC-OURANOS Collaborative
479 Research and Development grant (ARCHIVES project of INRS-ETE), and the Environmental
480 Geoscience Program of the Geological Survey of Canada (ESS contribution number
481 20140213).

482 **References**

- 483 Anchukaitis, K. J., D'Arrigo, R. D., Andreu-Hayles, L., Frank, D., Verstege, A., Curtis, A., Buckley, B.
484 M., Jacoby, G. C., and Cook, E. R.: Tree-ring reconstructed summer temperatures from
485 northwestern North America during the last nine centuries, *Journal of climate*, 10.1175/jcli-d-11-
486 00139.1, 2012.
- 487 Arseneault, D., Dy, B., Gennaretti, F., Autin, J., and Bégin, Y.: Developing millennial tree ring
488 chronologies in the fire-prone North American boreal forest, *J. Quat. Sci.*, 28, 283-292,
489 10.1002/jqs.2612, 2013.
- 490 Barber, V. A., Juday, G. P., Finney, B. P., and Wilmking, M.: Reconstruction of summer temperatures
491 in interior Alaska from tree-ring proxies: evidence for changing synoptic climate regimes, *Clim.*
492 *Change*, 63, 91-120, 2004.
- 493 Bard, E., Raisbeck, G. M., Yiou, F., and Jouzel, J.: Solar modulation of cosmogenic nuclide production
494 over the last millennium: comparison between¹⁴C and¹⁰Be records,
495 *Earth and Planetary Science Letters*, 150, 453-462, 1997.
- 496 Bard, E., Raisbeck, G.M., Yiou, F., Jouzel, J.: Solar modulation of cosmogenic nuclide production over
497 the last millennium: comparison between¹⁴C and¹⁰Be records. *Earth*
498 *and Planetary Science Letters*, 150(3): 453-462, 1997.
- 499 Bard, E., Raisbeck, G., Yiou, F., and Jouzel, J.: Reconstructed Solar Irradiance Data. IGBP
500 PAGES/World Data Center for Paleoclimatology Data Contribution Series #2003-006.
501 NOAA/NGDC Paleoclimatology Program, Boulder CO, USA, 2003.
- 502 Bard, E., and Frank, M.: Climate change and solar variability: What's new under the sun?. *Earth and*
503 *Planetary Science Letters*, 248(1), 1-14, 2006.
- 504 Boettger, T., and Friedrich, M.: A new serial pooling method of shifted tree ring blocks to construct
505 millennia long tree ring isotope chronologies with annual resolution, *Isot. Environ. Health Stud.*, 45,
506 68-80, 10.1080/10256010802522218, 2009.
- 507 Boulanger, Y., Gauthier, S., Burton, P. J., and Vaillancourt, M.-A.: An alternative fire regime zonation
508 for Canada, *International Journal of Wildland Fire*, 21, 1052-1064,
509 <http://dx.doi.org/10.1071/WF11073>, 2012.
- 510 Breitenmoser, P., Beer, J., Broennimann, S., Frank, D., Steinhilber, F., and Wanner, H.: Solar and
511 volcanic fingerprints in tree-ring chronologies over the past 2000years, *Palaeogeography*,
512 *Palaeoclimatology, Palaeoecology*, 313, 127-139, 2012.
- 513 Briffa, K. R., Jones, P. D., Schweingruber, F. H., and Osborn, T. J.: Influence of volcanic eruptions on
514 Northern Hemisphere summer temperature over the past 600 years, *Nature*, 393, 450-455, 1998.
- 515 Buishand, T.A. Some methods for testing the homogeneity of rainfall data. *Journal of Hydrology*, 58:
516 11-27, 1982.
- 517 Crowley, T. J.: Causes of climate change over the past 1000 years, *Science*, 289, 270-277, 2000.
- 518 Crowley, T.J. and Unterman, M. B.: Technical details concerning development of a 1200-yr proxy
519 index for global volcanism. *Earth System Science Data*, Vol. 5, pp. 187-197, DOI: 10.5194/essd-5-
520 187-2013, 2012.
- 521 Dai, J., Mosley-Thompson, E. and Thompson, L.G., 1991. Ice core evidence for an explosive tropical
522 volcanic eruption 6 years preceding Tambora. *Journal of Geophysical Research: Atmospheres*
523 (1984–2012), 96(D9): 17361-17366.
- 524 D'Arrigo, R., Jacoby, G. C., Wilson, R., Liepert, B., and Cherubini, P.: On the 'Divergence Problem' in
525 Northern Forests: A review of the tree-ring evidence and possible causes, *Global and Planetary*
526 *Change*, 60, 289-305, 10.1016/j.gloplacha.2007.03.004, 2008.
- 527 D'Arrigo, R. D., and Jacoby, G. C.: Northern North American tree-ring evidence for regional
528 temperature changes after major volcanic events, *Clim. Change*, 41, 1-15, 1999.Daux, V., Edouard,
529 J.-L., Masson-Delmotte, V., Stievenard, M., Hoffmann, G., Pierre, M., Mestre, O., Danis, P., and

530 Guibal, F.: Can climate variations be inferred from tree-ring parameters and stable isotopes from
531 *Larix decidua*? Juvenile effects, budmoth outbreaks, and divergence issue, *Earth and Planetary*
532 *Science Letters*, 309, 221-233, 2011.

533 Daux, V., Edouard, J. L., Masson-Delmotte, V., Stievenard, M., Hoffmann, G., Pierre, M., Mestre, O.,
534 Danis, P.A. and Guibal, F.: Can climate variations be inferred from tree-ring parameters and stable
535 isotopes from *Larix decidua*? Juvenile effects, budmoth outbreaks, and divergence issue. *Earth and*
536 *Planetary Science Letters*, 309(3), 221-233, 2011.

537 Ding, Q., Wallace, J.M., Battisti, D.S., Steig, E.J., Gallant, A.J., Kim, H.-J. and Geng, L.: Tropical
538 forcing of the recent rapid Arctic warming in north-eastern Canada and Greenland. *Nature*,
539 509(7499): 209-212, 2014.

540 Dorado Liñán, I., Gutiérrez, E., Helle, G., Heinrich, I., Andreu-Hayles, L., Planells, O., Leuenberger,
541 M., Bürger, C., and Schleser, G.: Pooled versus separate measurements of tree-ring stable isotopes,
542 *Science of the Total Environment*, 409, 2244-2251, 10.1016/j.scitotenv.2011.02.010, 2011.

543 Driscoll, W. W., Wiles, G. C., D'Arrigo, R. D., and Wilmking, M.: Divergent tree growth response to
544 recent climatic warming, Lake Clark National Park and Preserve, Alaska, *Geophys. Res. Lett.*, 32,
545 2005.

546 Edwards, T. W., Birks, S. J., Luckman, B. H., and MacDonald, G. M.: Climatic and hydrologic
547 variability during the past millennium in the eastern Rocky Mountains and northern Great Plains of
548 western Canada, *Quaternary Research*, 70, 188-197, 2008.

549 Esper, J., Frank, D. C., Timonen, M., Zorita, E., Wilson, R. J., Luterbacher, J., Holzkämper, S., Fischer,
550 N., Wagner, S., and Nievergelt, D.: Orbital forcing of tree-ring data, *Nature Climate Change*, 2, 862-
551 866, 2012.

552 Feng, S., Hu, Q., and Oglesby, R. J.: Influence of Atlantic sea surface temperatures on persistent
553 drought in North America, *Climate Dynamics*, 37, 569-586, 2011.

554 Fortin, D., and Lamoureux, S. F.: Multidecadal hydroclimatic variability in north-eastern North
555 America since 1550 AD, *Climate dynamics*, 33, 427-432, 2009.

556 Gagen, M., Zorita, E., McCarroll, D., Young, G. H. F., Grudd, H., Jalkanen, R., Loader, N. J.,
557 Robertson, I., and Kirchhefer, A.: Cloud response to summer temperatures in Fennoscandia over the
558 last thousand years, *Geophys. Res. Lett.*, 38, L0570110.1029/2010gl046216, 2011.

559 Gagen, M., McCarroll, D., Jalkanen, R., Loader, N. J., Robertson, I., and Young, G. H. F.: A rapid
560 method for the production of robust millennial length stable isotope tree ring series for climate
561 reconstruction, *Global and Planetary Change*, 82-83, 96-103,
562 <http://dx.doi.org/10.1016/j.gloplacha.2011.11.006>, 2012.

563 Gajewski, K., and Atkinson, D.: Climatic change in northern Canada, *Environmental Reviews*, 11, 69-
564 102, 2003.

565 Gao, C., Robock, A., and Ammann, C.: Volcanic forcing of climate over the past 1500 years: An
566 improved ice core-based index for climate models, *Journal of Geophysical Research: Atmospheres*
567 (1984-2012), 113, 2008.

568 Gennaretti, F., Arseneault, D., and Bégin, Y.: Millennial stocks and fluxes of large woody debris in
569 lakes of the North American taiga, *Journal of Ecology*, 102(2), 367-380, 2014a.

570 Gennaretti, F., Arseneault, D., Nicault, A., Perreault, L., and Bégin, Y.: Volcano-induced regime shifts
571 in millennial tree-ring chronologies from North-eastern North America, *Proceedings of the National*
572 *Academy of Sciences of the United States of America*, 111(28), 10077-10082, 2014b.

573 Gennaretti, F., Arseneault D. et Bégin, Y. : Millennial disturbance-driven forest stand dynamics in the
574 Eastern Canadian taiga reconstructed from subfossil logs, *Journal of Ecology*, 2014c.

575 Green, J. W.: Wood cellulose, *Methods in Carbohydrate Chemistry* III, 9-21, 1963.

576 Guiot, J., and Nicault, A.: Méthodes de dendroclimatologie à l'échelle continentale: fonctions de
577 réponse et fonction de transfert, *La dendroécologie*, 229-253, 2011.

578 Haupt, M., Friedrich, M., Shishov, V. V., and Boettger, T.: The construction of oxygen isotope
579 chronologies from tree-ring series sampled at different temporal resolution and its use as climate
580 proxies: statistical aspects, *Clim. Change*, 122, 201-215, 2014.

581 Hegerl, G. C., Crowley, T. J., Allen, M., Hyde, W. T., Pollack, H. N., Smerdon, J., and Zorita, E.:
582 Detection of human influence on a new, validated 1500-year temperature reconstruction, *Journal of*
583 *Climate*, 20, 650-666, 2007.

584 Helama, S., Lindholm, M., Timonen, M., J., M., and Eronen, M.: The supra-long Scots pine tree-ring
585 record for Finnish Lapland: Part 2, interannual to centennial variability in summer temperatures for
586 7500 years, *Holocene*, 12, 681-687, 2002.

587 Hurrell, J. W., Kushnir, Y., Ottersen, G., and Visbeck, M.: The North Atlantic Oscillation: climatic
588 significance and environmental impact, *American Geophysical Union*, 2003.

589 IPCC: Climatic change 2013: The physical Science Basis., Contribution of working group 1 to the fifth
590 assessment report of the intergovernmental panel on climate change, 2013.

591 Jacoby, G. C., Workman, K. W., and D'Arrigo, R. D.: Laki eruption of 1783, tree rings, and disaster
592 for northwest Alaska Inuit, *Quat. Sci. Rev.*, 18, 1365-1371, 1999.

593 Jones, G. S., Gregory, J. M., Stott, P. A., Tett, S. F., and Thorpe, R. B.: An AOGCM simulation of the
594 climate response to a volcanic super-eruption, *Climate Dynamics*, 25, 725-738, 2005.

595 Kaufman, D. S., Schneider, D. P., McKay, N. P., Ammann, C. M., Bradley, R. S., Briffa, K. R., Miller,
596 G. H., Otto-Bliesner, B. L., Overpeck, J. T., and Vinther, B. M.: Recent warming reverses long-term
597 Arctic cooling, *Science*, 325, 1236-1239, 2009.

598 Keller, C. F.: 1000 Years of climate change. *Advances in Space Research*, 34(2), 315-322, 2004.

599 Kobashi, T., Kawamura, K., Severinghaus, J. P., Barnola, J. M., Nakaegawa, T., Vinther, B. M.,
600 Johnsen, S. J., and Box, J. E.: High variability of Greenland surface temperature over the past 4000
601 years estimated from trapped air in an ice core, *Geophys. Res. Lett.*, 38, 2011.

602 Kobashi, T., Kawamura, K., Severinghaus, J. P., Barnola, J. M., Nakaegawa, T., Vinther, B. M.,
603 Johnsen, S. J., and Box, J. E.: GISP2 Ice Core 4000 Year Ar-N Isotope Temperature Reconstruction.
604 IGBP PAGES/World Data Center for Paleoclimatology Data Contribution Series # 2012-034.
605 NOAA/NCDC Paleoclimatology Program, Boulder CO, USA, 2012.

606 Landrum, L., Otto-Bliesner, B. L., Wahl, E. R., Conley, A., Lawrence, P. J., Rosenbloom, N., and
607 Teng, H.: Last Millennium Climate and Its Variability in CCSM4, *Journal of Climate*, 26, 2013.

608 Lean, J., Beer, J., and Bradley, R.: Reconstruction of solar irradiance since 1610: Implications for
609 climate change, *Geophysics Research Letter*, 22, 3195-3198, 1995.

610 Ljungqvist, F., Krusic, P. J., Brattström, G., and Sundqvist, H. S.: Northern Hemisphere temperature
611 patterns in the last 12 centuries, *Climate of the Past*, 8, 2012.

612 Loader, N., Young, G. H., McCarroll, D., and Wilson, R. J.: Quantifying uncertainty in isotope
613 dendroclimatology, *The Holocene*, 2013a.

614 Loader, N. J., Robertson, I., Barker, A. C., Switsur, V. R., and Waterhouse, J. S.: An improved
615 technique for the batch processing of small wholewood samples to [alpha]-cellulose, *Chemical*
616 *Geology*, 136, 313-317, Doi: 10.1016/s0009-2541(96)00133-7, 1997.

617 Loader, N. J., Young, G. H. F., Grudd, H., and McCarroll, D.: Stable carbon isotopes from Torneträsk,
618 northern Sweden provide a millennial length reconstruction of summer sunshine and its relationship

619 to Arctic circulation, *Quat. Sci. Rev.*, 62, 97-113, <http://dx.doi.org/10.1016/j.quascirev.2012.11.014>,
620 2013b.

621 Luckman, B.H. and Wilson, R.J.S.: Canadian Rockies Summer Temperature Reconstruction. IGBP
622 PAGES/World Data Center for Paleoclimatology. Data Contribution Series # 2006-011.
623 NOAA/NCDC Paleoclimatology Program, Boulder CO, USA, 2006.

624 Luckman, B., and Wilson, R.: Summer temperatures in the Canadian Rockies during the last
625 millennium: a revised record, *Climate Dynamics*, 24, 131-144, 2005.

626 Mann, M. E., Zhang, Z., Rutherford, S., Bradley, R. S., Hughes, M. K., Shindell, D., Ammann, C.,
627 Faluvegi, G., and Ni, F.: Global signatures and dynamical origins of the Little Ice Age and Medieval
628 Climate Anomaly, *Science*, 326, 1256-1260, 2009.

629 Masson-Delmotte, V., Schulz, M., Abe-Ouchi, A., Beer, J., Ganopolski, A., González Rouco J.F.,
630 Jansen, E., Lambeck, K., Luterbacher, J., Naish, T., Osborn, T., Otto-Bliesner, B., Quinn, T.,
631 Ramesh, R., Rojas, M., Shao, X. and Timmermann, A.: Information from Paleoclimate Archives. In:
632 *Climate Change 2013: The Physical Science Basis. Contribution of Working Group I to the Fifth*
633 *Assessment Report of the Intergovernmental Panel on Climate Change* [Stocker, T.F., D.Qin, G.-K.
634 Plattner, M. Tignor, S.K. Allen, J. Boschung, A. Nauels, Y. Xia, V. Bex and P.M. Midgley (eds.)].
635 Cambridge University Press, Cambridge, United Kingdom and New York, NY, USA, pp. 383–464,
636 2013. doi:10.1017/CBO9781107415324.013.

637 McCarroll, D., and Loader, N. J.: Stable isotopes in tree rings, *Quat. Sci. Rev.*, 23, 771-801,
638 10.1016/j.quascirev.2003.06.017, 2004.

639 Miller, G.H., Geirsdottir, A., Zhong, Y., Larsen, D.J., Otto-Bliesner, B.L., Holland, M.M., Bailey,
640 D.A., Refsnider, K.A., Lehman, S.J. and Southon, J.R.: Abrupt onset of the Little Ice Age triggered
641 by volcanism and sustained by sea-ice/ocean feedbacks. *Geophysical research letters*, 39(2), 2012.

642 Moberg, A., Sonechkin, D. M., Holmgren, K., Datsenko, N. M., and Karlén, W.: Highly variable
643 Northern Hemisphere temperatures reconstructed from low-and high-resolution proxy data, *Nature*,
644 433, 613-617, 2005.

645 Moore, J., Hughen, K., Miller, G., and Overpeck, J.: Little Ice Age recorded in summer temperature
646 reconstruction from varved sediments of Donard Lake, Baffin Island, Canada, *Journal of*
647 *Paleolimnology*, 25, 503-517, 2001.

648 Naulier, M., Savard, M. M., Bégin, C., Marion, J., Arseneault, D., and Bégin, Y.: Carbon and oxygen
649 isotopes of lakeshore black spruce trees in north-eastern Canada as proxies for climatic
650 reconstruction, *Chemical Geology*, 374, 37-43, 2014.

651 Naulier, M.: Développement de séries isotopiques et reconstitution des conditions climatiques estivales
652 du dernier millénaire à partir de tiges subfossiles dans le nord de la forêt boréale Québécoise, Ph.D.
653 thesis, Institut National de la Recherche Scientifique – Eau Terre Environnement, Canada, 237pp.,
654 available at : <http://espace.inrs.ca/2610/1/NaulierMaud.pdf>, 2015.

655 Naulier, M., Savard, M.M., Bégin, C., Marion, J., Nicault, A., and Bégin, Y.: Temporal instability of
656 isotopes-climate statistical relationships- A study of black spruce trees in northeastern Canada,
657 *Dendrochronologia*, in press.

658 PAGES 2k consortium, P. K.: Continental-scale temperature variability during the past two millennia,
659 *Nature geoscience*, doi:10.1038/NGEO1797, 2013.

660 Payette, S., Filion, L., Delwaide, A., and Bégin, C.: Reconstruction of tree-line vegetation response to
661 long-term climate change, *Nature*, 341, 429-432, 1989.

662 Plummer, C., Curran, M., van Ommen, T., Rasmussen, S.O., Moy, A., Vance, T., Clausen, H.B.,
663 Vinther, B.M. and Mayewski, P.: An independently dated 2000-yr volcanic record from Law Dome,
664 East Antarctica, including a new perspective on the dating of the 1450s CE eruption of Kuwae,
665 Vanuatu. *Climate of the Past*, 8(6): 1929-1940, 2012.

666 Porter, T., Pisaric, M. J., Field, R., Kokelj, S., Edwards, T. D., deMontigny, P., Healy, R., and
667 LeGrande, A.: Spring-summer temperatures since AD 1780 reconstructed from stable oxygen

isotope ratios in white spruce tree-rings from the Mackenzie Delta, northwestern Canada, *Climate Dynamics*, 1-15, 10.1007/s00382-013-1674-3, 2013.

Robertson, I., Switsur, V.R., Carter, A.H.C., Barker, A.C., Waterhouse, J.S., Briffa, K.R., Jones, P.D.: Signal strength and climate relationships in $^{13}\text{C}/^{12}\text{C}$ ratios of tree ring cellulose from oak in east England. *J. Geophys. Res.*, 102(D16): 19507-19516, 1997.

Rinne, K. T., Boettger, T., Loader, N. J., Robertson, I., Switsur, V. R., and Waterhouse, J. S.: On the purification of [alpha]-cellulose from resinous wood for stable isotope (H, C and O) analysis, *Chemical Geology*, 222, 75-82, DOI: 10.1016/j.chemgeo.2005.06.010, 2005.

Savard, M. M., Bégin, C., Marion, J., Arseneault, D., and Bégin, Y.: Evaluating the integrity of C and O isotopes in sub-fossil wood from boreal lakes, *Palaeogeography, Palaeoclimatology, Palaeoecology*, 348–349, 21-31, <http://dx.doi.org/10.1016/j.palaeo.2012.06.003>, 2012.

Shindell, D. T., Schmidt, G. A., Miller, R. L., and Mann, M. E.: Volcanic and solar forcing of climate change during the preindustrial era, *Journal of Climate*, 16, 4094-4107, 2003.

Sicre, M. A., Weckström, K., Seidenkrantz, M. S., Kuijpers, A., Benetti, M., Massé, G., Ezat, U., Schmidt, S., Bouloubassi, I., Olsen, J., Khodri, M. and Mignot, J.: Labrador current variability over the last 2000 years. *Earth and Planetary Science Letters*, 400, 26-32, 2014.

Sigl, M., McConnell, J. R., Layman, L., Maselli, O., McGwire, K., Pasteris, D., Dorthé, D.J., Steffensen, B.V., Edwards, R., Mulvaney, R. & Kipfstuhl, S.A.: New bipolar ice core record of volcanism from WAIS Divide and NEEM and implications for climate forcing of the last 2000 years. *Journal of Geophysical Research: Atmospheres*, 118(3), 1151-1169, 2013.

Thomas, E.K. and Briner, J.P.: Big Round Lake, Baffin Island Varve Thickness Data. IGBP PAGES/World Data Center for Paleoclimatology Data Contribution Series # 2008-115. NOAA/NCDC Paleoclimatology Program, Boulder CO, USA, 2008.

Thomas, E. K., and Briner, J. P.: Climate of the past millennium inferred from varved proglacial lake sediments on northeast Baffin Island, Arctic Canada, *Journal of Paleolimnology*, 41, 209-224, 2009.

Thomas, S. R., Owens, M. J., and Lockwood, M.: The 22-Year Hale Cycle in Cosmic Ray Flux—Evidence for Direct Heliospheric Modulation, *Solar Physics*, 289, 407-421, 2014.

Tingley, M. P., Stine, A. R. and Huybers, P.: Temperature reconstructions from tree-ring densities overestimate volcanic cooling. *Geophysical Research Letters*, 41(22), 7838-7845, 2014.

Trouet, V., Esper, J., Graham, N. E., Baker, A., Scourse, J. D., and Frank, D. C.: Persistent positive North Atlantic Oscillation mode dominated the medieval climate anomaly, *Science*, 324, 78-80, 2009.

Trouet, V., Scourse, J., and Raible, C.: North Atlantic storminess and Atlantic Meridional Overturning Circulation during the last millennium: reconciling contradictory proxy records of NAO variability, *Global and Planetary Change*, 84, 48-55, 2012.

Trouet, V., Diaz, H., Wahl, E., Viau, A., Graham, R., Graham, N., and Cook, E.: A 1500-year reconstruction of annual mean temperature for temperate North America on decadal-to-multidecadal time scales, *Environmental Research Letters*, 8, 024008, 2013.

Viau, A., and Gajewski, K.: Reconstructing millennial-scale, regional paleoclimates of boreal Canada during the Holocene, *Journal of Climate*, 22, 2009.

Viau, A., Ladd, M., and Gajewski, K.: The climate of North America during the past 2000 years reconstructed from pollen data, *Global and Planetary Change*, 84, 75-83, 2012.

Vinther, B.M., Buchardt, S.L., Clausen, H.B., Dahl-Jensen, D., Johnsen S.J., Fisher, D.A., Koerner, R.M., Raynaud, D., Lipenkov, V., Andersen, K.K., Blunier, T., Rasmussen, S.O., Steffensen, J.P., and Svensson, A.M.: Holocene shinning of the greenland ice sheet. *Nature*, Vol. 461, pp. 385-388, 2009.

Vinther, B.M., Buchardt, S.L., Clausen, H.B., Dahl-Jensen, D., Johnsen S.J., Fisher, D.A., Koerner, R.M., Raynaud, D., Lipenkov, V., Andersen, K.K., Blunier, T., Rasmussen, S.O., Steffensen, J.P., and Svensson, A.M.: Greenland Ice Sheet Holocene $\delta^{18}\text{O}$, Temperature, and Surface Elevation.

717 IGBP PAGES/World Data Center for Paleoclimatology Data Contribution Series # 2011-053.
718 NOAA/NCDC Paleoclimatology Program, Boulder CO, USA, 2011.
719 Vinther, B. M., Jones, P. D., Briffa, K. R., Clausen, H. B., Andersen, K. K., Dahl-Jensen, D., and
720 Johnsen, S. J.: Climatic signals in multiple highly resolved stable isotope records from Greenland.
721 Quaternary Science Reviews, 29(3), 522-538, 2010.
722 Way, R. G., and Viau, A. E.: Natural and forced air temperature variability in the Labrador region of
723 Canada during the past century. Theoretical and Applied Climatology, 1-12, 2014.
724 Wood, G.D.A: Tambora: The Eruption That Changed the World. Princeton University Press, 2014.
725 Young, G.H.F., McCarroll, D., Loader, N.J. and Kirchhefer, A.J.: A 500-year record of summer near-
726 ground solar radiation from tree-ring stable carbon isotopes. Holocene, 20(3): 315-324, 2010.

Figures and table

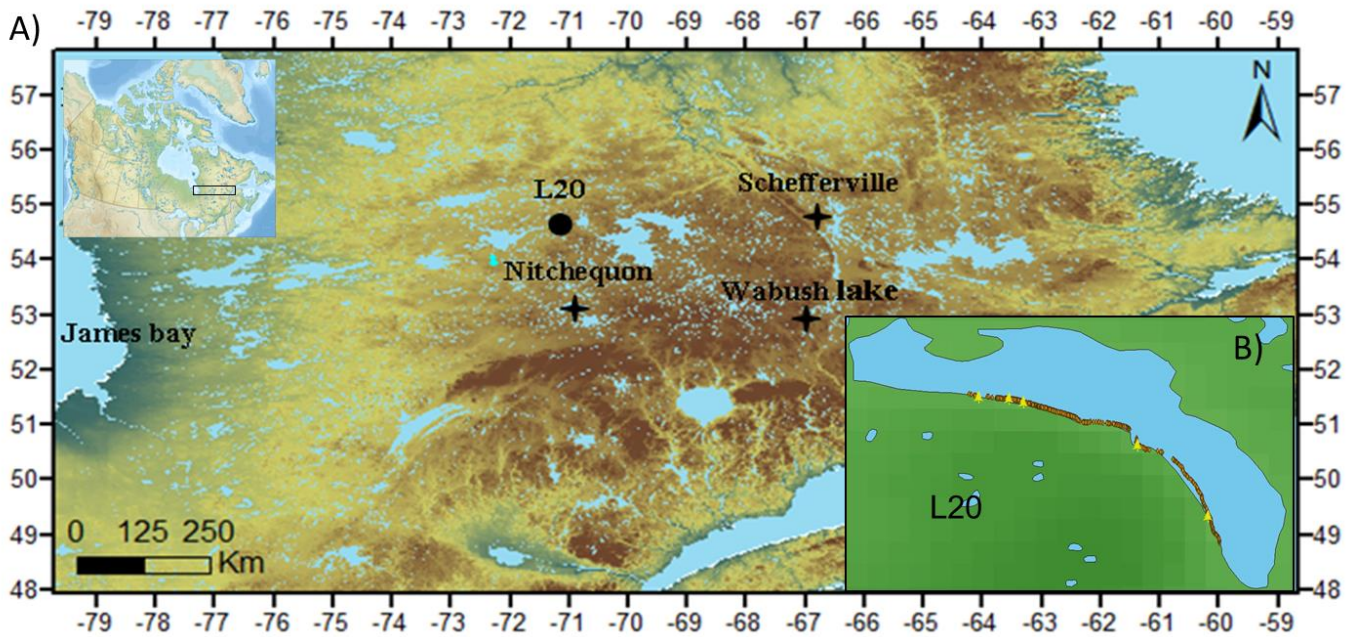


Figure 1. A) Site location (black circle) and meteorological stations (black stars). B) Representation of lake L20, also illustrating the sampling location of subfossil stems (brown marks) and living trees (yellow marks).

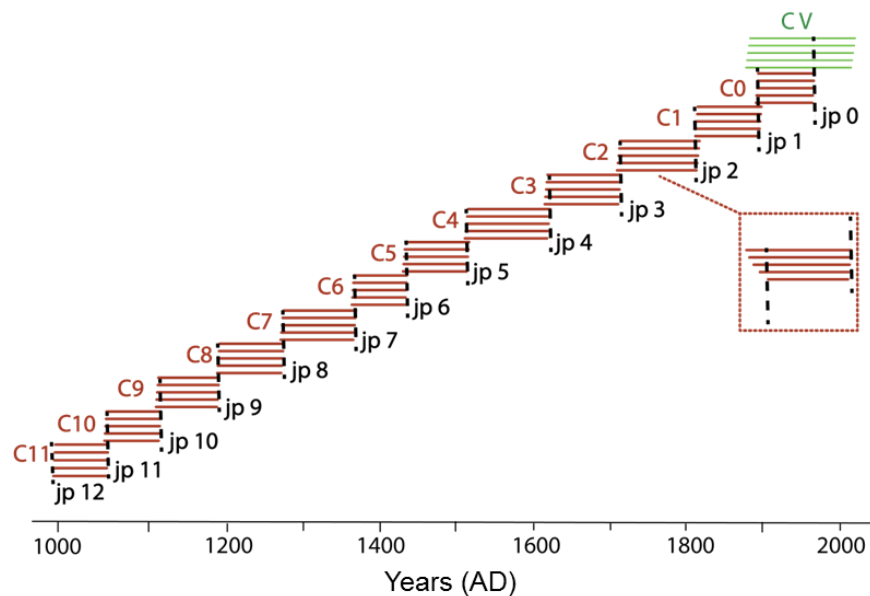
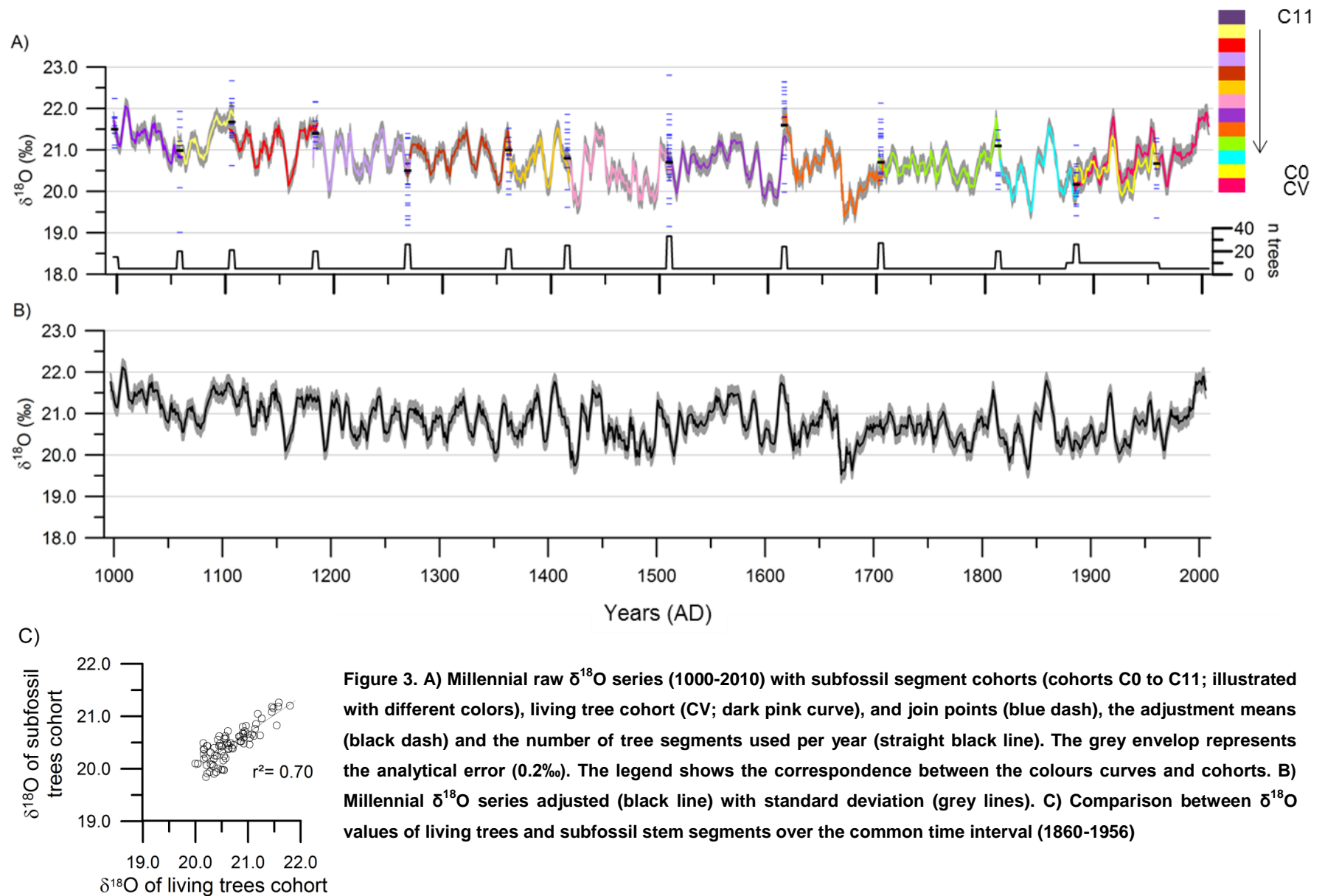


Figure 2. Illustration of the sampling strategy. From year 1000 to 2006, cohorts are represented in red for subfossil stem segments (C0-C11), and in green for living trees (CV). The join points are in black on the overlapping periods (JP0 to JP12).



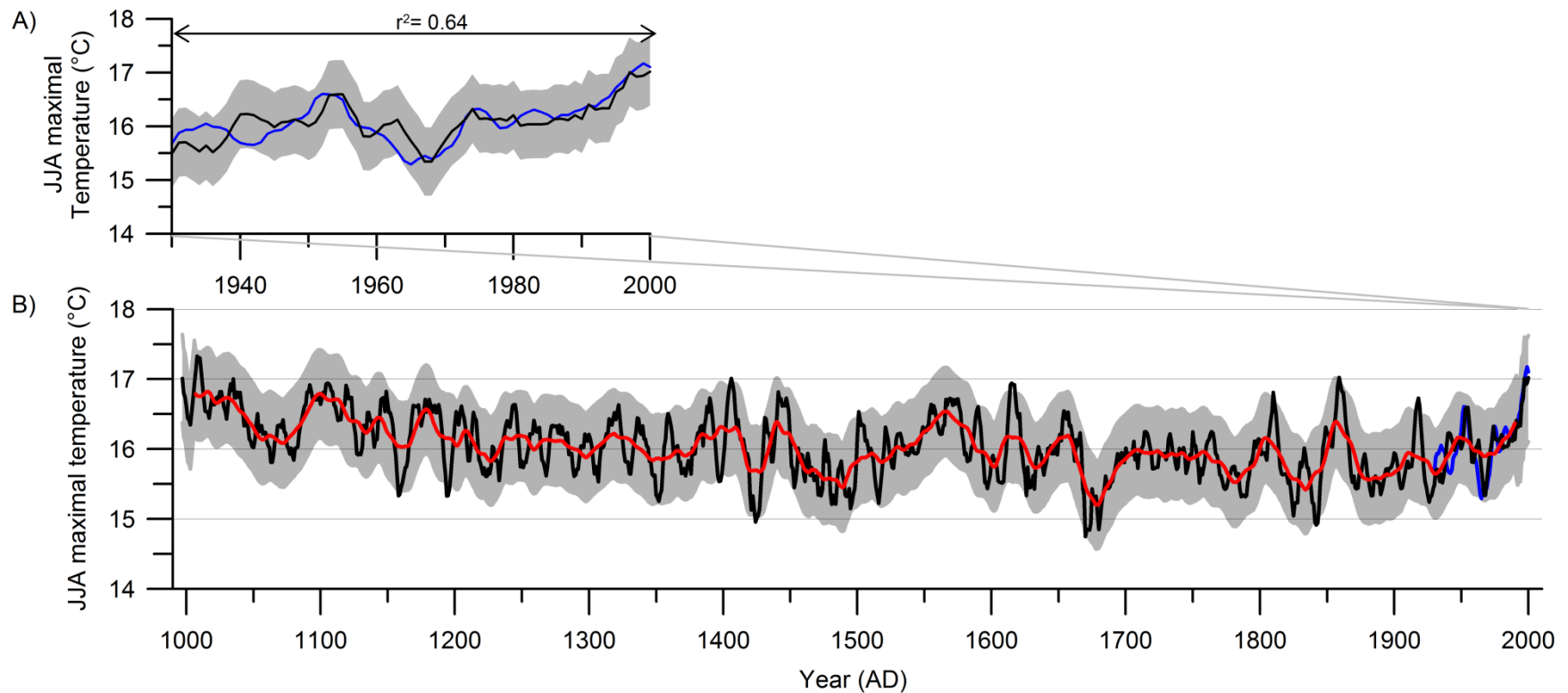


Figure 4. A) Comparison between reconstructed (i-STREC, black line) and observed (blue line) JJA maximal temperature and mean square values on the entire period of calibration. **B)** i-STREC (black line) with 21-year moving average (red line) and observed JJA maximal temperature series from CRU TS3.1 (blue line). In both cases, the dark grey shading represents uncertainty with ± 1 RMSE calculated on the 21-year filter values.

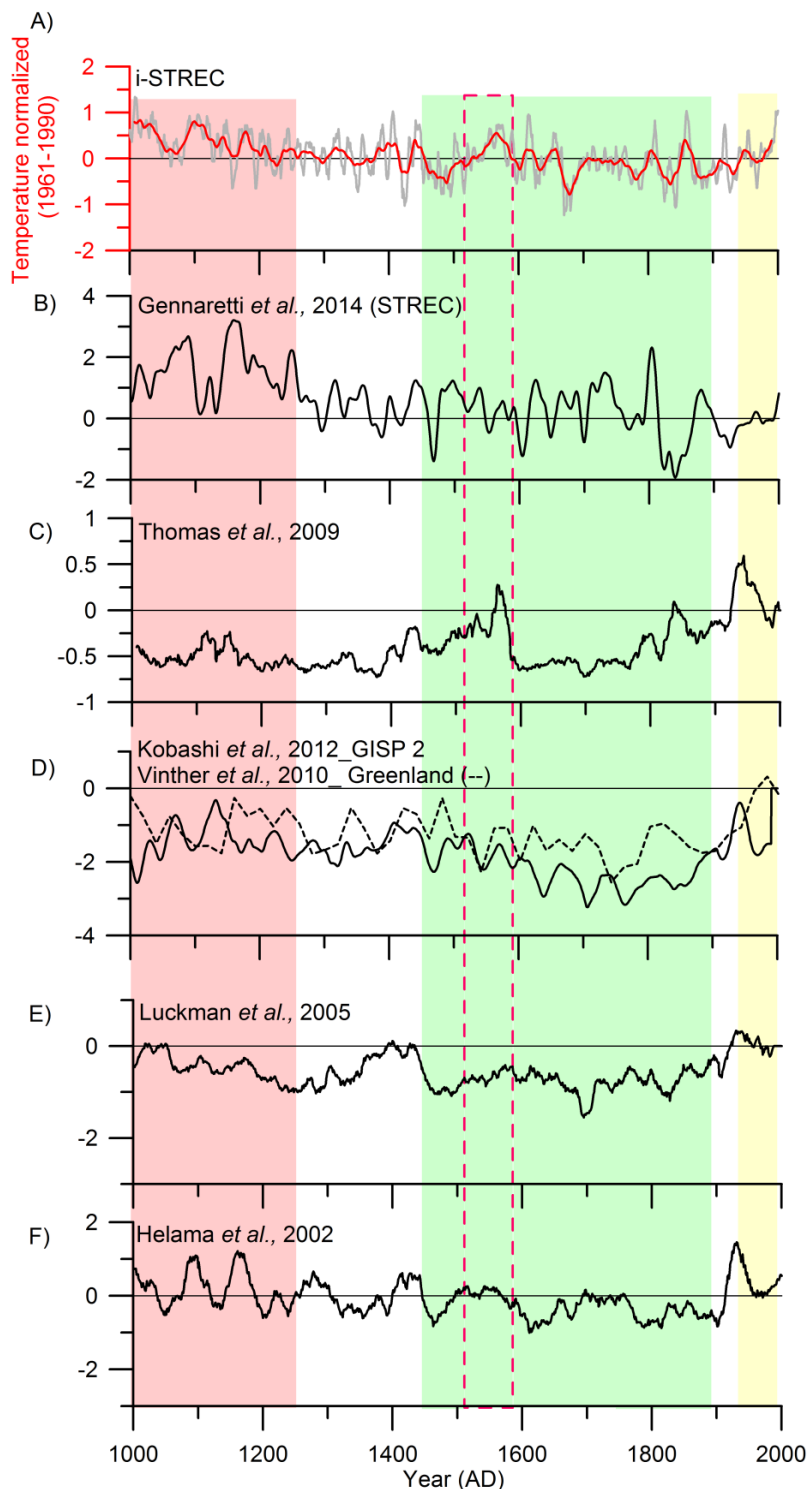


Figure 5. Comparison between i-STREC and other temperature reconstructions (data obtained from NOAA). (A) i-STREC from in north-eastern Canada. B) STREC from tree-ring width, in the same region. C) July-September temperature from varved sediments, Baffin Island, Arctic Canada. D) annual surface temperature from GISP 2 ice core, in Greenland. E) May-August maximum temperature from maximum latewood density and tree-ring width, Canadian Rockies. F) July temperature from tree-ring width, northern Finland. Shading based on i-STREC is shown to ease comparison with the other reconstructions compiled: warmer (pink, colder (green) and modern periods (yellow). All reconstructions have been smoothed with a 21-years filter and normalized (1960-1991).

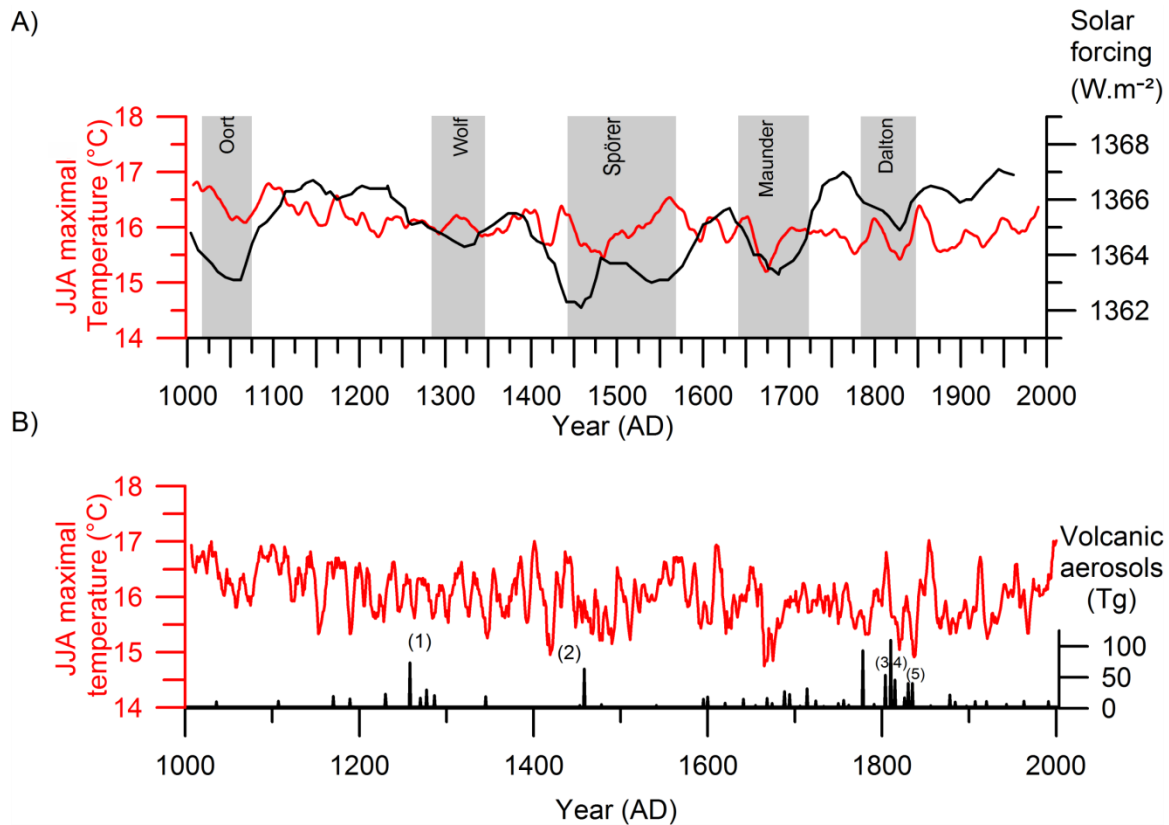


Figure 6. Volcanic and solar forcings. A) I-STREC (reconstructed summer temperature, 21-years smoothed; red line), compared with the well-known solar minima (grey bands) and the solar forcing series (black line; Bard *et al.*, 2003). B) I-STREC reconstructed summer temperature (red line) compared with the volcanic aerosols sulfates (Sigl *et al.*, 2013). The major eruptions are marked: (1) 1257/1258= Samalas, (2) 1456= Kuwae, (3) 1783= Laki, (4) 1809= unknown and 1815= Tambora and (5) 1835= Cosigüina).

1 Table 1. Summary of the verification statistics for calibrations using the linear scaling and simple
 2 linear regression methods for different periods, and using the measured maximal temperature
 3 series.

	Calibration (1930-1970) Linear scaling/ simple linear regression	Calibration (1971-2000) Linear scaling/ simple linear regression	Calibration (1930-2000) Linear scaling/ simple linear regression
Average °C± SD	15.9 ± 0.3	16.4 ± 0.4	16.1 ± 0.4
R ² calibration	0.27/ 0.43	0.85/ 0.85	
R ² verification	0.85/ 0.85	0.27/ 0.43	
R ² total period			0.62/ 0.64
RMSE verification, °C	0.14/ 0.33	0.34/ 0.33	
RMSE calibration, °C	0.33/ 0.16	0.15/ 0.14	
RMSE total period, °C			0.27/ 0.25
RE	0.94/ 0.19	0.64/ 0.07	0.57/ 0.64
CE	0.84/ 0.05	-0.02/ 0.21	0.57/ 0.64

4 SD is the standard deviation, r² is the coefficient of determination (R squared), RMSE the raw
 5 mean squared error, RE the reduction of error and CE the coefficient of error.